




## Charge ordering mechanism in silver difluoride

Mariana Derzsi <sup>1,\*</sup>, Kamil Tokár <sup>1,2</sup>, Przemysław Piekarczyk <sup>3</sup>, and Wojciech Grochala<sup>4</sup>

<sup>1</sup>*Advanced Technologies Research Institute, Faculty of Materials Science and Technology in Trnava, Slovak University of Technology in Bratislava, J. Bottu 25, 917 24 Bratislava, Trnava, Slovakia*

<sup>2</sup>*Institute of Physics, Slovak Academy of Sciences, Dúbravská cesta 9, 845 11 Bratislava, Slovakia*

<sup>3</sup>*Institute of Nuclear Physics, Polish Academy of Sciences, Radzikowskiego 152, 31342 Kraków, Poland*

<sup>4</sup>*Center of New Technologies, University of Warsaw, Zwirki i Wigury 93, 02089 Warsaw, Poland*



(Received 24 August 2021; accepted 14 February 2022; published 24 February 2022)

Using density functional theory, a competition between the Mott-Hubbard and intervalence charge transfer mechanism of electron localization is revealed in  $\text{AgF}_2$ , an important silver analog of oxocuprates. We show that at reduced temperature and electron correlations  $\text{AgF}_2$  becomes metallic and dynamically unstable with respect to soft phonon modes that promote charge ordering. The charge density wave (CDW) instability is closely related to the Kohn anomaly and Fermi surface nesting. The long advocated  $\text{KBrF}_4$ -type CDW  $\text{Ag}^{1+/3+}\text{F}_2$  structure and its facile transformation to the ground state  $\text{Ag}^{2+}\text{F}_2$  phase is explained. Our results point to an intimate interplay between lattice, charge, and spin degrees of freedom in this seemingly simplistic binary metal fluoride.

DOI: [10.1103/PhysRevB.105.L081113](https://doi.org/10.1103/PhysRevB.105.L081113)

Copper oxide superconductors exhibit a number of competing phases when the antiferromagnetic (AFM) Mott insulating state is doped by charges [1,2]. Since the first observation of the striped phase in  $\text{CuO}_2$  planes [3], growing evidence of charge order (CO) existing in all families of cuprates has been accumulated [4–7]. In most cases, low-temperature CO phases are observed at moderate doping levels and they are characterized by a two-dimensional (2D) charge density wave (CDW) with a modulation vector  $q_{\text{CDW}}$  [8]. The CDW is stabilized by ionic displacements and often accompanied by a phonon anomaly observed at the wave vector  $q_{\text{CDW}}$  [9,10], thus showing similar behavior as prototypical CDW systems [11,12]. Despite extensive studies, understanding of CO formation and its role in high- $T_c$  superconductivity is still far from complete due to the complexity of materials, doping dependence, chemical disorder, and many-body effects [8,13].

It was demonstrated that  $\text{AgF}_2$ , also known as  $\alpha$ - $\text{AgF}_2$  (*Pbca*), is an excellent silver analog of the parent compound of high- $T_c$  superconducting cuprates [14]. It consists of layers of spin-1/2 ions with a formally  $\text{Ag}(d^9)$  electronic configuration—unpaired electrons reside in the  $d_{x^2-y^2}$  orbitals and couple antiferromagnetically via a superexchange mechanism that involves  $F(p)$  orbitals [14,15]. In contrast to the flat  $\text{CuO}_2$  layers in cuprates, the neutral layers forming a square lattice in  $\text{AgF}_2$  are severely buckled [16–18]. Elimination of the buckling could result in an AFM coupling that surpasses the cuprates [15]. Assuming a magnetically driven mechanism, such large coupling could potentially lead to superconducting critical temperatures higher than those exhibited by cuprates [19].

The most recent experimental and theoretical study on the interband excitations in  $\text{AgF}_2$  demonstrates that  $\text{AgF}_2$  is at

the verge of a charge transfer instability [20], while independent experimental studies reported the observation of a metastable diamagnetic  $\beta$  phase interpreted as charge-ordered  $\text{Ag}^{1+}\text{Ag}^{3+}\text{F}_4$  that fast-transforms to the  $\alpha$ - $\text{Ag}^{2+}\text{F}_2$  structure [21]. It was proposed that  $\beta$ - $\text{AgF}_2$  takes on the  $\text{KBrF}_4$ -type structure with *I4/mcm* symmetry [21–23] and indeed a recent theoretical study demonstrated the dynamical stability of  $\text{AgF}_2$  in a  $\text{KBrF}_4$  lattice [24]. It was also explained that orthorhombic  $\alpha$  and  $\text{KBrF}_4$ -type  $\beta$  phases both emerge from fluorite-type structures via a distinct order parameter, i.e., freezing out a different phonon mode [24]. The  $\text{Ag}^{2+}\text{F}_2$  layers formed by the edge sharing of square-planar [ $\text{Ag}^{2+}\text{F}_4$ ] units in the  $\alpha$  phase are disintegrated and replaced by layers of isolated square planar [ $\text{Ag}^{3+}\text{F}_4$ ] units and  $\text{Ag}^{1+}$  cations alternating along the tetragonal  $c$  direction in a  $\text{KBrF}_4$ -type lattice. Despite the above-described differences, both crystal structures are intimately related and differ only in displacements of the fluorine atoms, while the volume of the  $\text{KBrF}_4$ -type unit cell is doubled relative to the  $\alpha$  phase. This is reminiscent of the situation in the oxocuprates, where the charge- and spin-ordered domains are related by displacements of oxygen atoms in the  $\text{CuO}_2$  layers [13].

The existence of the  $\beta$  phase and its transformation to  $\alpha$  clearly point to competing AFM and CDW orders with different mechanisms of electron localization in  $\text{AgF}_2$ . Furthermore, it suggests that the CO phase is metastable relative to the spin-ordered AFM phase and quickly destroyed thermally via intervalence charge transfer (IVCT),  $\text{Ag}^{1+} + \text{Ag}^{3+} \rightarrow 2\text{Ag}^{2+}$ . Most importantly, it indicates that the CO  $\text{AgF}_2$  phase may be stabilized already in an undoped regime in contrast to the superconducting copper oxides, where the CO appears at moderate doping levels.

The main goal of this Letter is to investigate the mechanism of charge ordering in  $\text{AgF}_2$  and its possible relation to the Kohn anomaly and Fermi surface nesting. We show that at reduced temperatures and electron correlations  $\alpha$ - $\text{AgF}_2$

\*Corresponding author: mariana.derzsi@stuba.sk

becomes metallic and dynamically unstable with respect to CDW phonon modes that promote CO. We also show that the long advocated  $\text{KBrF}_4$ -type structure of the observed charge-ordered  $\beta\text{-AgF}_2$  naturally emerges from the  $\alpha$  phase due to a phonon-induced CDW state when the exact exchange is accounted for within the hybrid Heyd-Scuseria-Ernzerhof (HSE) functional. Our study shows that the transition from the AFM to CO state via the metallic state in  $\text{AgF}_2$  involves electron-phonon coupling enhanced by Fermi surface nesting. It also reveals the importance of electron correlations for the stabilization of both the spin- and the charge-ordered  $\text{AgF}_2$  phases.

In the present studies, the electronic and crystal structure of the studied systems have been optimized using the density functional theory (DFT) implemented in the Vienna *ab initio* simulation package (VASP) [25]. Lattice parameters and atomic positions were fully relaxed using the projector augmented-wave method [26] and the generalized gradient approximation (GGA) of Perdew-Burke-Ernzerhof optimized for solids (PBEsol) [27] were used. The energy cutoff was set to 520 eV. The occupations of electronic states close to the Fermi energy were smeared by the Gaussian method with  $\sigma = 0.05$  eV. The strong electron interactions in the  $\text{Ag}(4d)$  states have been included within the DFT +  $U$  method [28] with the Coulomb parameter  $U = 5.0$  eV and the Hund's exchange  $J = 1$  eV [29], and using the hybrid HSE06 functional with 25% of exact exchange [30]. For plotting the Fermi surfaces, the Wannier interpolation was performed on calculated electronic bands using the WANNIER90 software [31]. The phonon dispersion curves were obtained using the direct method [32] implemented in the program PHONOPY [33].

The proper insulating state with AFM order can be obtained in  $\alpha\text{-AgF}_2$  only if local electron interactions are included beyond the standard DFT approximation, within such methods as hybrid functionals or the DFT +  $U$  approach [15,24,34]. Recent progress in meta-GGA functionals [35] provides an alternative approach that can be applied also to  $\text{AgF}_2$ . The electronic band structure calculated with hybrid DFT shows an insulating gap of 2.3 eV [15]. A similar electronic state was obtained within the DFT +  $U$  method with a realistic value of the parameter  $U_{\text{Ag}} = 5$  eV [29], however, the band gap is about two times smaller (1.17 eV) [24]. Calculations of phonon dispersions performed by DFT +  $U$  show a dynamical stability of  $\alpha\text{-AgF}_2$  with the AFM ground state [17,24].

Within the GGA, the electronic state is metallic without any magnetic order and a phonon instability in the form of a sharp dip reminiscent of a Kohn anomaly develops at the Z point as it is shown in Fig. 1(a). This is a doubly degenerate mode with the dominant contribution of F atoms [see the Supplemental Material (SM)] [36]. Both phonon branches at the Z point cause bond disproportionation within the  $\text{AgF}_2$  layers due to the  $[\text{AgF}_4]$  breathing motion accompanied by doubling of the unit cell along the direction perpendicular to the layers (Fig. 2). While all four Ag-F bonds elongate for one silver atom, they contract for the nearest four silver atoms that share the same fluorine atoms. Consequently, all four Ag-F bonds shorten for half of the Ag atoms and elongate for the other half within the layer. At the positions with shortened bonds, the valence corresponds to  $\text{Ag}^{3+}$ , while

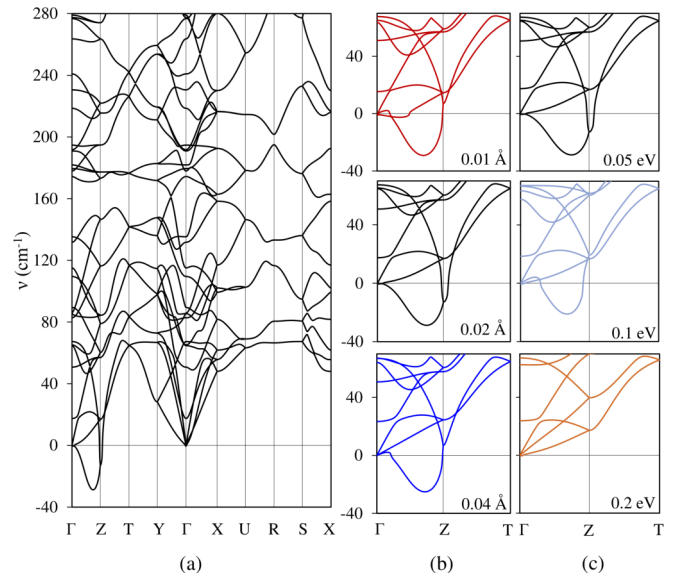


FIG. 1. Phonon dispersion relations in  $\text{AgF}_2$  obtained with the atomic displacement  $u = 0.02$  Å (a), and impact of the atomic displacement (b) and electron smearing width (c) on the C-CDW and I-CDW modes along the  $\Gamma$ -Z direction calculated for the nonmagnetic state with the GGA. The value of the displacement and the smearing width is indicated in the lower right corner of each plot in (b) and (c), respectively.

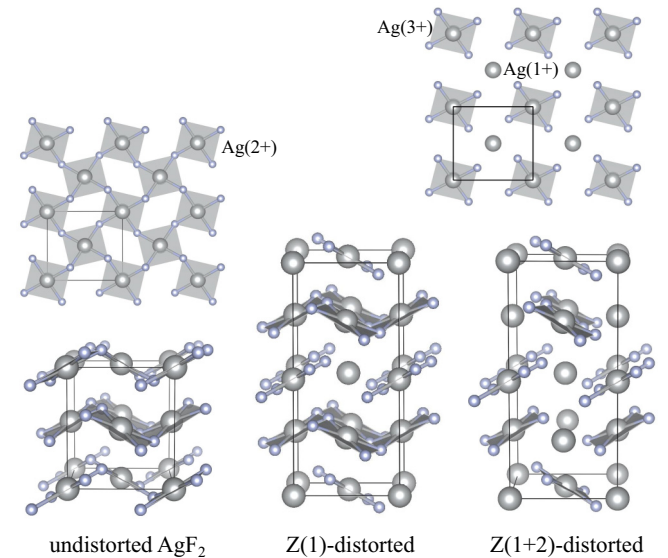


FIG. 2. Charge disproportionation and cell doubling induced by the doubly degenerate phonon mode at the Z point: undistorted  $\text{AgF}_2$  (left), and distorted by one Z(1) arm (AFM-CDW phase, middle) and both Z(1 + 2) arms of the Z mode (CDW phase, right). Large balls: Ag atoms; small balls: F atoms. Ag atoms for which no connections to F atoms are shown (middle and right panels) are those around which the intralayer Ag-F bonds are elongated by the Z mode. The remaining Ag-F bonds within the same layer are contracted. One  $\text{AgF}_2$  layer distorted by the Z mode is illustrated in the top right corner, which can be compared with an undistorted  $\text{AgF}_2$  layer shown in top left corner. The Ag valencies are also indicated.

at those with elongated bonds to  $\text{Ag}^{1+}$ . Thus, this breathing mode mediates CDW associated with the IVCT mechanism  $2\text{Ag}^{2+} \rightarrow \text{Ag}^{1+} + \text{Ag}^{3+}$ . Each single branch of the soft mode affects every second layer as is presented in the middle panel of Fig. 2. Since both modes make distortions in different layers, they together induce the IVCT in the entire crystal (Fig. 2, right panel). The commensurate CDW (C-CDW) instability [i.e., appearing at the high-symmetry Z point with commensurate vector  $q = (0, 0, 0.5)$ ] is accompanied by an even more imaginary incommensurate component (I-CDW) that develops along the  $\Gamma$ -Z direction with a minimum around  $q = (0, 0, 0.37)$  and causes the same intralayer atomic displacements as the C-CDW. The I-CDW mediates the IVCT in all  $\text{AgF}_2$  layers and simultaneously modulates the stacking of the charge-modulated  $\text{Ag}^{1+}\text{Ag}^{3+}\text{F}_4$  layers. The presence of the C-CDW indicates the existence of long-range ordering, which means that there is significant interplanar coupling, leading to the 3D CDW phase. The existence of the I-CDW component also indicates the possibility of competition between different incommensurate phases, which may destroy the long-range order.

A frequency of the C-CDW mode is highly sensitive to the amplitude of atomic displacements, showing nonmonotonic evolution with increasing amplitude [see Fig. 1(b)]. It first decreases and then increases, while it remains imaginary only for the intermediate amplitude ( $u = 0.02 \text{ \AA}$ ). On the other hand, the I-CDW branch along the  $\Gamma$ -Z direction shows almost no dependence on the amplitude and remains imaginary for all calculated values. The strong dependence of a phonon frequency on the amplitude of atomic displacement indicates its strong sensitivity to temperature, which is characteristic of a Kohn anomaly. More specifically, it increases with increasing temperature due to the smearing of the Fermi surface. Therefore, we have explored this dependence using the first-order Methfessel-Paxton and Gaussian smearing functions. Both the C-CDW and the I-CDW modes show a high sensitivity to the smearing width independent of the smearing function, and their frequencies increase with increasing smearing width as expected for a Kohn anomaly. The C-CDW mode becomes stabilized (with real frequencies) upon a slight increase of the smearing width from a value of 0.05 to 0.1 eV, while the I-CDW mode becomes stabilized at a higher value of 0.2 eV [Fig. 1(c)]. The above results suggest that metallic  $\text{AgF}_2$  would first transform to an I-CDW phase and subsequently to a C-CDW phase with decreasing temperature:  $\text{Ag}^{2+}\text{F}_2 \rightarrow \text{incommensurate Ag}^{1+/3+}\text{F}_2 \rightarrow \text{commensurate Ag}^{1+/3+}\text{F}_2$ .

A typical Kohn anomaly is observed at the phonon wave vector  $q$ , which is related to the Fermi wave vector  $k_F$  by the simple relation  $q = 2k_F$ . Such a wave vector connects points at the Fermi surface, and the effect is particularly strong if  $q$  connects large areas of the Fermi surface parallel to each other. This phenomenon is called nesting, and it plays a role behind the formation mechanism of CDW. In  $\text{AgF}_2$ , the Fermi surface of the metallic state (in the GGA limit) is composed of four bands that are partially filled below the Fermi level [Fig. 3(a)]. Figure 3(b) depicts a cross section of the Fermi surface of one of these bands with the Brillouin zone (BZ) face defined by the  $U$ - $X$ - $S$  plane containing a possible nesting vector  $q_Z = (0, 0, 0.5)$  connecting areas of the corner pockets

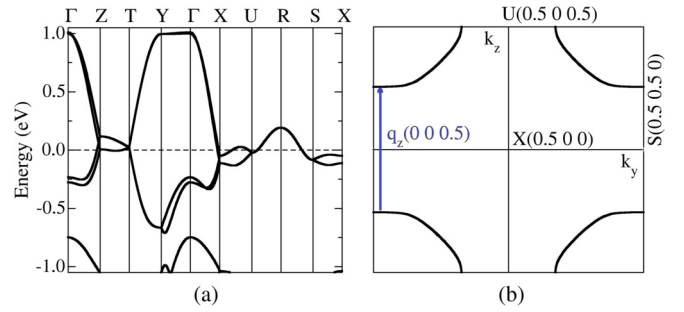


FIG. 3. Electronic band structure at the vicinity of the Fermi level (a) and the cross section of the Fermi surface along the  $U$ - $X$ - $S$  line (b) for the metallic  $\text{AgF}_2$  solution obtained with the GGA.

of the Fermi surface. In this cross section, we clearly observe the linear parts of the Fermi surface, which can be connected by the  $q_Z$  wave vector. This is consistent with the Kohn mechanism of the phonon softening at the Z point.

The charge density redistribution mediated by the soft mode at the Z point is evident from the observation of the atom-resolved electronic density of states (DOS) shown in Fig. 4(b). It reveals a distinct contribution from two neighboring silver atoms labeled in the DOS plot as Ag1 and Ag2. One can notice a decreased population of the lowest-energy valence and conduction states of Ag2 relative to Ag1 that indicates the formation of  $\text{Ag}^{1+}$  ( $d^{10}$ ) and  $\text{Ag}^{3+}$  (low-spin  $d^8$ ), respectively. The CDW is accompanied by the opening of a point gap at the Fermi level. The gap develops in the upper Hubbard  $\text{Ag}(d_{x^2-y^2})$  band that spreads between  $-1$  and  $1$  eV and is strongly hybridized with the  $p_x$  and  $p_y$  orbitals (not shown) [14,15]. Note that the partial segregation of the  $d_{x^2-y^2}$  band to a valence and a conduction band is already present in the undistorted metallic solution near the Fermi level [Fig. 4(a)].

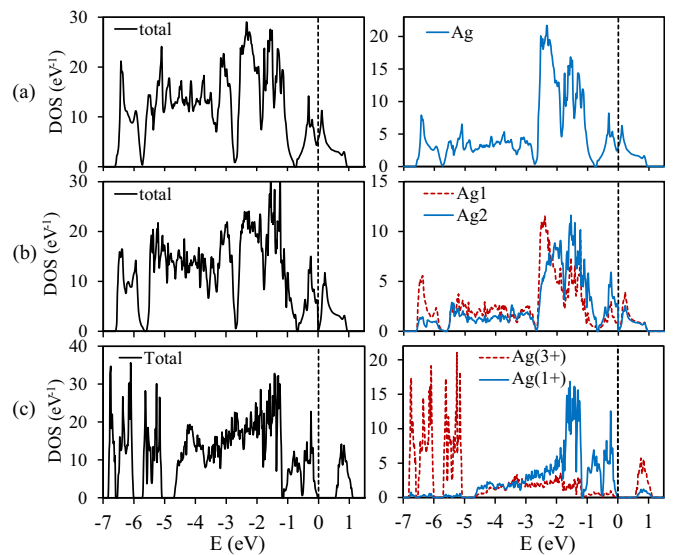


FIG. 4. Total and atom (Ag)-resolved density of states of undistorted  $\text{AgF}_2$  in the GGA regime (a), and distorted (optimized) structure along the imaginary Z mode of  $\text{AgF}_2$  in the GGA (b) and GGA +  $U$  regime with  $U_{\text{Ag}} = 5$  eV (c).

It is evident that charge disproportionation is only partial within the standard DFT picture, since  $\text{Ag}^{1+}$  cation requires full occupation of all  $d$  states, while in the distorted structure both Ag ions have partially depopulated  $d$  states. The charge disproportionation is further enhanced and a full band gap opens when the on-site electron interaction  $U$  is accounted for. The complete charge transfer  $2\text{Ag}^{2+} \rightarrow \text{Ag}^{1+} + \text{Ag}^{3+}$  takes place for a realistic value of  $U_{\text{Ag}} = 5$  eV as witnessed by the atom-resolved DOS in Fig. 4(c). All  $d$  states are now fully occupied for Ag2 and the  $d_{x^2-y^2}$  band is depopulated for Ag1 as expected for  $\text{Ag}^{1+}$  and low-spin  $\text{Ag}^{3+}$ , respectively.

We recall that each branch of the doubly degenerate CDW mode at the  $Z$  point leads to a local minimum, an intermediate between the AFM and the CO solution, with spin and charge domains distributed to alternating  $\text{Ag}^{2+}\text{F}_2$  and  $\text{Ag}^{1+/3+}\text{F}_2$  layers (Fig. 2, middle panel). In the  $\text{Ag}^{1+/3+}\text{F}_2$  layers the band gap opens by charge order while in the  $\text{Ag}^{2+}\text{F}_2$  by spin order via the AFM superexchange. The AFM state within the  $\text{Ag}^{2+}\text{F}_2$  layers can be obtained only if electron correlations beyond the standard GGA are accounted for [15,24,34]. Within DFT +  $U$ , it is stabilized for  $U \geq 1$  eV. The band gap in the AFM layers is larger than in the IVCT layers by a factor of 2 irrespective of the value of  $U$ . The coexistence of spin and charge domains in  $\text{AgF}_2$  is reminiscent of stripe phases in cuprates characterized by a unique distribution of spin and charge densities. In cuprates, however, the stripes form within the  $[\text{CuO}_2]$  layers [8,12].

It has been suggested that the CDW structure of  $\text{AgF}_2$  takes on the  $\text{KBrF}_4$  ( $\text{Na}^{1+}\text{Ag}^{3+}\text{F}_4$ ) type [21–24]. This structure requires doubling of the  $\alpha$ - $\text{AgF}_2$  unit cell, which correlates well with our theoretical result that reveals the soft mode at the  $Z$  point [Fig. 1(a)]. However, this mode leads to an orthorhombic  $Pca2_1$  structure with different ordering of the  $\text{Ag}^{1+}$  and  $\text{Ag}^{3+}$  ions and orientation of the square planar  $[\text{Ag}^{3+}\text{F}_4]$  units than the tetragonal  $\text{KBrF}_4$  type. The  $\text{KBrF}_4$ -type structure ensures perfect antiferrodistortive orientation of the units, which minimizes secondary  $\text{Ag}^{3+}\text{-F}\cdots\text{Ag}^{3+}$  interactions and maximizes splitting between the doubly occupied  $d_{z^2}$  and the empty  $d_{x^2-y^2}$  orbital. This leads to a further broadening of the band gap [compare Fig. 4(c) with the DOS of the  $\text{KBrF}_4$  type from Ref. [24]] and thus increased stability of the CO state by 27 meV/atom when considering  $U_{\text{Ag}} = 5$  eV. We have found that, when distorting the  $\text{AgF}_2$  lattice along the  $Z$  mode and optimizing it with the hybrid functional, it converges to the  $\text{KBrF}_4$ -type structure (the electron DOS is presented and compared with other calculations in the SM [36]). This result shows that the transition from the spin-ordered ground state to the charge-ordered ground state involves strong electron

correlations that are not sufficiently captured by the standard DFT and DFT +  $U$  functionals.

The results presented in this Letter indicate an essential role of lattice dynamics and electron-phonon coupling in  $\text{AgF}_2$ . The CDW mode at the  $Z$  point induces charge disproportionation on Ag ions. The band splitting in the vicinity of the Fermi level is caused solely by a lattice distortion as demonstrated by DFT with no local electron interaction  $U$  included. However, the fully charge-ordered state with a completely opened band gap is reached only when local interactions are taken into consideration within the DFT +  $U$  approach. Inclusion of the exact exchange in the form of a hybrid HSE functional drives further atomic displacements in the CO state towards the  $\text{KBrF}_4$ -type ground state structure with a larger splitting of the  $e_g$  orbitals that provides additional stabilization. Since the total energy of this phase is higher than the ground state energy of the AFM  $\alpha$  phase [24] (see the SM [36]), the  $\beta$ - $\text{AgF}_2$  structure must be treated as metastable. It explains a fast  $\beta \rightarrow \alpha$  transformation observed experimentally [21].

In this Letter we discussed the phonon-driven mechanism of electron localization, which competes with the AFM interactions and promotes charge disproportionation in  $\text{AgF}_2$ . We revealed the soft mode related to the Kohn anomaly enhanced by Fermi surface nesting. Uncovering the CDW mechanism underneath the AFM spin ordering (that prevails at realistic values of on-site electron correlations) gives us an important hint that one could potentially tune the electronic structure between these two regimes (charge ordering versus spin ordering), for example, by strain or alloying.

M.D. and K.T. acknowledge the European Regional Development Fund, Research and Innovation Operational Program (ITMS2014 +: 313011 W085), the Slovak Research and Development Agency (APVV-18-0168), and Scientific Grant Agency of the Slovak Republic (VG 1/0223/19). P.P. acknowledges the support by Narodowe Centrum Nauki (NCN, National Science Centre, Poland), Project No. 2017/25/B/ST3/02586. W.G. acknowledges Polish National Science Center (NCN) for Beethoven project (2016/23/G/ST5/04320). The research was carried out using the Aurel supercomputing infrastructure in CC of Slovak Academy of Sciences acquired within the projects ITMS 26230120002 and ITMS 26210120002 (Slovak infrastructure for high-performance computing) supported by the Research & Development Operational Program funded by the ERDF, and infrastructure of Centre for Mathematical and Computational Modelling (ICM), University of Warsaw (Grants No. G62-24, No. GA83-34).

- [1] E. Fradkin, S. A. Kivelson, and J. M. Tranquada, Colloquium: Theory of intertwined orders in high temperature superconductors, *Rev. Mod. Phys.* **87**, 457 (2015).
- [2] B. Keimer, S. A. Kivelson, M. R. Norman, S. Uchida, and J. Zaanen, From quantum matter to high-temperature superconductivity in copper oxides, *Nature (London)* **518**, 179 (2015).
- [3] J. M. Tranquada, B. J. Sternlieb, J. D. Axe, Y. Nakamura, and S. Uchida, Evidence for stripe correlations of spins and holes

in copper oxide superconductors, *Nature (London)* **375**, 561 (1995).

- [4] J. Chang, E. Blackburn, A. T. Holmes, N. B. Christensen, J. Larsen, J. Mesot, R. Liang, D. A. Bonn, W. N. Hardy, A. Watenphul, M. v. Zimmermann, E. M. Forgan, and S. M. Hayden, Direct observation of competition between superconductivity and charge density wave order in  $\text{YBa}_2\text{Cu}_3\text{O}_{6.67}$ , *Nat. Phys.* **8**, 871 (2012).

- [5] R. Comin, A. Frano, M. M. Yee, Y. Yoshida, H. Eisaki, E. Schierle, E. Weschke, R. Sutarto, F. He, A. Soumyanarayanan, Y. He, M. Le Tacon, I. S. Elfimov, J. E. Hoffman, G. A. Sawatzky, B. Keimer, and A. Damascelli, Charge order driven by Fermi-arc instability in  $\text{Bi}_2\text{Sr}_{2-x}\text{La}_x\text{CuO}_{6+\delta}$ , *Science* **343**, 390 (2014).
- [6] W. Tabis, Y. Li, M. Le Tacon, L. Braicovich, A. Kreyssig, M. Minola, G. Della, E. Weschke, M. J. Veit, M. Ramazanoglu, A. I. Goldman, T. Schmitt, G. Ghiringhelli, N. Barišić, M. K. Chan, C. J. Dorow, G. Yu, X. Zhao, B. Keimer, and M. Greven, Charge order and its connection with Fermi-liquid charge transport in a pristine high- $T_c$  cuprate, *Nat. Commun.* **5**, 5875 (2014).
- [7] E. H. da Silva Neto, R. Comin, F. He, R. Sutarto, Y. Jiang, R. L. Greene, G. A. Sawatzky, and A. Damascelli, Charge ordering in the electron-doped superconductor  $\text{Nd}_{2-x}\text{Ce}_x\text{CuO}_4$ , *Science* **347**, 282 (2015).
- [8] A. Frano, S. Blanco-Canosa, B. Keimer, and R. J. Birgeneau, Charge ordering in superconducting copper oxides, *J. Phys.: Condens. Matter* **32**, 374005 (2020).
- [9] M. Le Tacon, A. Bosak, S. M. Souliou, G. Della, T. Loew, R. Heid, K.-P. Bohnen, G. Ghiringhelli, M. Krisch, and B. Keimer, Inelastic x-ray scattering in  $\text{YBa}_2\text{Cu}_3\text{O}_{6.6}$  reveals giant phonon anomalies and elastic central peak due to charge-density-wave formation, *Nat. Phys.* **10**, 52 (2014).
- [10] H. Miao, D. Ishikawa, R. Heid, M. Le Tacon, G. Fabbris, D. Meyers, G. D. Gu, A. Q. R. Baron, and M. P. M. Dean, Incommensurate Phonon Anomaly and the Nature of Charge Density Waves in Cuprates, *Phys. Rev. X* **8**, 011008 (2018).
- [11] F. Weber, S. Rosenkranz, J.-P. Castellan, R. Osborn, R. Hott, R. Heid, K.-P. Bohnen, T. Egami, A. H. Said, and D. Reznik, Extended Phonon Collapse and the Origin of the Charge-Density Wave in  $2H\text{-NbSe}_2$ , *Phys. Rev. Lett.* **107**, 107403 (2011).
- [12] Q. Zhang, L.-Y. Gan, Y. Cheng, and U. Schwingenschlög, Spin polarization driven by a charge-density wave in monolayer  $1T\text{-TaS}_2$ , *Phys. Rev. B* **90**, 081103(R) (2014).
- [13] Y. Zhang, C. Lane, J. W. Furness, B. Barbiellini, J. P. Perdew, R. S. Markiewicz, A. Bansil, and J. Sun, Competing stripe and magnetic phases in the cuprates from first principles, *Proc. Natl. Acad. Sci. USA* **117**, 68 (2020).
- [14] W. Grochala and R. Hoffmann, Real and hypothetical intermediate-valence  $\text{Ag}^{\text{II}}/\text{Ag}^{\text{III}}$  and  $\text{Ag}^{\text{II}}/\text{Ag}^{\text{I}}$  fluoride systems as potential superconductors, *Angew. Chem., Int. Ed.* **40**, 2742 (2001).
- [15] J. Gawraczyński, D. Kurzydłowski, R. A. Ewings, S. Bandaru, W. Gadomski, Z. Mazej, G. Ruani, I. Bergenti, T. Jaroń, A. Ozarowski, S. Hill, P. J. Leszczyński, K. Tokár, M. Derzsi, P. Barone, K. Wohlfeld, J. Lorenzana, and W. Grochala, Silver route to cuprate analogs, *Proc. Natl. Acad. Sci. USA* **116**, 1495 (2019).
- [16] P. Fischer, D. Schwarzenbach, and H. M. Rietveld, Crystal and magnetic structure of silver difluoride: I. Determination of the  $\text{AgF}_2$  structure, *J. Phys. Chem. Solids* **32**, 543 (1971).
- [17] A. Grzelak, J. Gawraczyński, T. Jaroń, D. Kurzydłowski, A. Budzianowski, Z. Mazej, P. J. Leszczyński, V. B. Prakapenka, M. Derzsi, V. V. Struzhkin, and W. Grochala, High-pressure behavior of silver fluorides up to 40 GPa, *Inorg. Chem.* **56**, 14651 (2017).
- [18] I. Sánchez-Movellán, J. Moreno-Ceballos, P. García-Fernández, J. A. Aramburu, and M. Moreno, New ideas for understanding the structure and magnetism in  $\text{AgF}_2$ : Prediction of ferroelasticity, *Chem. - Eur. J.* **27**, 1 (2021).
- [19] A. Grzelak, H. Su, X. Yang, D. Kurzydłowski, J. Lorenzana, and W. Grochala, Epitaxial engineering of flat silver fluoride cuprate analogs, *Phys. Rev. Materials* **4**, 084405 (2020).
- [20] N. Bachar, K. Koterias, J. Gawraczyński, W. Trzeński, J. Paszula, R. Piombo, P. Barone, Z. Mazej, G. Ghiringhelli, A. Nag, K.-J. Zhou, J. Lorenzana, D. van der Marel, and W. Grochala, Charge transfer and  $dd$  excitations in  $\text{AgF}_2$ , [arXiv:2105.08862](https://arxiv.org/abs/2105.08862).
- [21] C. Shen, B. Žemva, G. M. Lucier, O. Graudejus, J. A. Allman, and N. Bartlett, Disproportionation of  $\text{Ag}(\text{II})$  to  $\text{Ag}(\text{I})$  and  $\text{Ag}(\text{III})$  in fluoride systems and syntheses and structures of  $(\text{AgF}^+)_2\text{AgF}_4^-\text{MF}_6^-$  salts ( $M = \text{As}, \text{Sb}, \text{Pt}, \text{Au}, \text{Ru}$ ), *Inorg. Chem.* **38**, 4570 (1999).
- [22] B. G. Müller, Fluorides of copper, silver, gold, and palladium, *Angew. Chem., Int. Ed. Engl.* **26**, 1081 (1987).
- [23] O. Graudejus, A. P. Wilkinson, and N. Bartlett, Structural features of  $\text{Ag}[\text{AuF}_4]$  and  $\text{Ag}[\text{AuF}_6]$  and the structural relationship of  $\text{Ag}[\text{AgF}_4]_2$  and  $\text{Au}[\text{AuF}_4]_2$  to  $\text{Ag}[\text{AuF}_4]_2$ , *Inorg. Chem.* **39**, 1545 (2000).
- [24] K. Tokár, M. Derzsi, and W. Grochala, Comparative computational study of antiferromagnetic and mixed-valent diamagnetic phase of  $\text{AgF}_2$ : Crystal, electronic and phonon structure and  $p$ - $T$  phase diagram, *Comput. Mater. Sci.* **188**, 110250 (2021).
- [25] G. Kresse and J. Furthmüller, Efficient iterative schemes for *ab initio* total-energy calculations using a plane-wave basis set, *Phys. Rev. B* **54**, 11169 (1996).
- [26] P. E. Blöchl, Projector augmented-wave method, *Phys. Rev. B* **50**, 17953 (1994).
- [27] J. P. Perdew, A. Ruzsinszky, G. I. Csonka, O. A. Vydrov, G. E. Scuseria, L. A. Constantin, X. Zhou, and K. Burke, Restoring the Density-Gradient Expansion for Exchange in Solids and Surfaces, *Phys. Rev. Lett.* **100**, 136406 (2008).
- [28] A. I. Liechtenstein, V. I. Anisimov, and J. Zaanen, Density-functional theory and strong interactions: Orbital ordering in Mott-Hubbard insulators, *Phys. Rev. B* **52**, R5467 (1995).
- [29] D. Kasinathan, K. Koepf, U. Nitzsche, and H. Rosner, Ferromagnetism Induced by Orbital Order in the Charge-Transfer Insulator  $\text{Cs}_2\text{AgF}_4$ : An Electronic Structure Study, *Phys. Rev. Lett.* **99**, 247210 (2007).
- [30] A. V. Krukau, O. A. Vydrov, A. F. Izmaylov, and G. E. Scuseria, Influence of the exchange screening parameter on the performance of screened hybrid functionals, *J. Chem. Phys.* **125**, 224106 (2006).
- [31] G. Pizzi, V. Vitale, R. Arita, S. Blügel, F. Freimuth, G. Géranton, M. Gibertini, D. Gresch, C. Johnson, T. Koretsune, J. Ibañez-Azpiroz, H. Lee, J.-M. Lihm, D. Marchand, A. Marrazzo, Y. Mokrousov, J. I. Mustafa, Y. Nohara, Y. Nomura, L. Paulatto *et al.*, Wannier90 as a community code: new features and applications, *J. Phys.: Condens. Matter* **32**, 165902 (2020).
- [32] K. Parlinski, Z. Q. Li, and Y. Kawazoe, First-Principles Determination of the Soft Mode in Cubic  $\text{ZrO}_2$ , *Phys. Rev. Lett.* **78**, 4063 (1997).
- [33] A. Togo and I. Tanaka, First principles phonon calculations in materials science, *Scr. Mater.* **108**, 1 (2015).
- [34] D. Kurzydłowski, M. Derzsi, P. Barone, A. Grzelak, V. Struzhkin, J. Lorenzana, and W. Grochala, Dramatic enhancement of spin-spin coupling and quenching of

- magnetic dimensionality in compressed silver difluoride, *Chem. Commun.* **54**, 10252 (2018).
- [35] B. Patra, S. Jana, L. A. Constantin, and P. Samal, Relevance of the Pauli kinetic energy density for semilocal functionals, *Phys. Rev. B* **100**, 155140 (2019).
- [36] See Supplemental Material at <http://link.aps.org/supplemental/10.1103/PhysRevB.105.L081113> for details about the electronic density of states and energetics for undistorted and distorted  $\text{AgF}_2$  with various DFT functionals as well as the phonon density of states in the region of imaginary frequencies.